THE TROPICAL WARM POOL INTERNATIONAL CLOUD EXPERIMENT

BY PETER T. MAY, JAMES H. MATHER, GERAINT VAUGHAN, CHRISTIAN JAKOB, GREG M. MCFARQUHAR, KEITH N. BOWER, AND GERALD G. MACE

A comprehensive observing campaign in Darwin, including a ship, five aircraft, and frequent soundings, is furthering weather and climate change studies through improved understanding and modeling of cloud and aerosol processes in tropical cloud systems.

A crucial factor in our ability to forecast future climate change is a better representation of tropical cloud systems, and their heating and radiative impacts in climate models (Stephens 2005; Del Genio and Kovari 2002; Neale and Slingo 2003; Spencer and Slingo 2003). This requires a better understanding of the factors that control tropical convection as well as an improved understanding of how the characteristics of the convection affect the nature of the cloud particles that are found in deep convective anvils and tropical cirrus. Deep convection also lifts boundary layer air into the tropical tropopause layer (TTL), affecting the composition of this region and through it the global stratosphere (e.g., Russell et al. 1993; Folkins 2002). Understanding the transport of gases and particles in deep convection is also therefore of global importance.

As a response to this challenge, a major field experiment named the Tropical Warm Pool International Cloud Experiment (TWP-ICE), including the U.K. Aerosol and Chemical Transport in Tropical Convection (ACTIVE) consortium, was undertaken in the Darwin, Northern Australia, area in January and February 2006. The experiment was designed to provide a comprehensive dataset for the development of cloud remote-sensing retrievals and initial-

AFFILIATIONS: MAY—Centre for Australian Weather and Climate Research, Australian Bureau of Meteorology and CSIRO, Melbourne, Australia; JAKOB—School of Mathematical Sciences, Monash University, Clayton, Australia; MATHER—Pacific Northwest National Laboratory, Richland, Washington; VAUGHAN AND BOWER—School of Earth, Atmospheric and Environmental Sciences, University of Manchester, Manchester, United Kingdom; MCFARQUHAR—Department of Atmospheric Sciences, University of Illinois at Urbana–Champaign Urbana, Illinois; MACE—Meteorology Department, University of Utah, Salt Lake City, Utah
A supplement to this article is available online (DOI:10.1175/BAMS-89-5-May)

CORRESPONDING AUTHOR: Peter T. May, Centre for Australian Weather and Climate Research, Australian Bureau of Meteorology and CSIRO, GPO Box 1289, Melbourne 3001, Australia
E-mail: p.may@bom.gov.au

The abstract for this article can be found in this issue, following the table of contents.

DOI:10.1175/BAMS-89-5-629

In final form 31 October 2007
©2008 American Meteorology Society

izing and verifying a range of process-scale models (e.g., Blossey et al. 2007), with a view to improve the parameterization of tropical convection and clouds in numerical weather prediction and climate models. Accordingly, a surface measurement network (including a research ship) was combined with a fleet of five research aircraft to enable in situ and remote-sensing measurements of clouds, meteorological variables, and composition from the ground into the lower stratosphere. A key feature was the dense sounding array on the scale of a GCM grid box with 3-hourly balloon launches throughout the campaign.

A key goal of the research being conducted with TWP-ICE data is to understand and model the link between the properties of the atmosphere on the scale of a typical GCM grid box and the strength and organization of convection as well as the resulting characteristics of the accompanying cloud field, in particular cirrus. Aerosol measurements followed on from those made by ACTIVE in the pre-Christmas campaign (Vaughan et al. 2008) to document the evolution of the atmosphere from that with substantial impact from biomass burning at the end of the dry season to pristine conditions in late January.

The TWP-ICE design built on such experiments as the Global Atmospheric Research Program (GARP) Atlantic Tropical Experiment (GATE); (Houze and Betts 1981), Winter Monsoon Experiment (W-MONEX; Greenfield and Krishnamurti 1979), Australian Monsoon Experiment (AMEX)/Equatorial Mesoscale Experiment (EMEX; Holland et al. 1986; Webster and Houze 1991), Tropical Ocean and Global Atmosphere Coupled Ocean–Atmosphere Response Experiment (TOGA COARE; Webster and Lukas 1992), Central Equatorial Pacific Ocean Experiment (CEPEX; Heymsfield and McFarquhar 1996), and Tropical Rainfall Measuring Mission (TRMM) Kwajalein Experiment (KWAJEX; Yuter et al. 2005). These experiments described various elements of convective cloud systems and their interaction with the large-scale circulation. Many aspects of their approaches have been combined, particularly the combination of a dense sounding network combined with high-altitude aircraft as well as airborne and ground-based radar and lidar. Cloud-sampling strategies employed during TWP-ICE built on previous experiments such as the Cirrus Regional Study of Tropical Anvils and Cirrus Layers–Florida-Area Cirrus Experiment (CRYSTAL-FACE; Garrett et al. 2005; Heymsfield et al. 2005), which emphasized the physical and chemical properties of cirrus and the upper-troposphere region.

Darwin experiences a wide variety of convective systems, including those typical of a monsoon coastal environment, similar to those experienced by large populations under the influence of the Asian and Indian monsoons (e.g., Keenan and Carbone 1992; Cecil et al. 2005; Nesbitt et al. 2006). Monsoon cloud systems are typically oceanic in character, and some of the lessons of TWP-ICE can be applied across tropical oceanic areas, including the intertropical convergence zone (ITCZ). The monsoon exhibits very high intraseasonal variability (e.g., Drosdowsky 1996) and experiences both active periods with storms typical of a maritime environment and "breaks" when the storm systems are characteristic of coastal and continental areas. These break storms have high lightning activity and are often isolated, forming on sea breezes and other local circulations, although some of these ultimately develop into squall lines. This is in contrast to the widespread, but generally weaker convective activity sampled during the active phase of the monsoon (e.g., Mapes and Houze 1992; Keenan and Carbone 1992; May and Ballinger 2007). The TWP-ICE period sampled both of these regimes as well as a relatively suppressed period with storms of only moderate vertical extent. Furthermore, similar cloud regimes, as objectively identified from an analysis of International Satellite Cloud Climatology Project (ISCCP) data across the western Pacific by Jakob and Tselioudis (2003), are seen in Darwin across the tropics (Höglund 2005).

Darwin hosts what is probably the most comprehensive long-term meteorological observational network anywhere in the tropics. This network is described in the "Ground network observations" section and provides long-term datasets so that the TWP-ICE data can be put into a climatological context. This is particularly important given the limited duration of the TWP-ICE intensive observing period.

The combination of excellent facilities and the range of tropical weather experienced have made for a long history of field programs in the Darwin area. Important examples of these were the combined AMEX/EMEX/Stratosphere–Troposphere Exchange Program (STEP) in the late 1980s, focusing on the structure of the Australian monsoon and the potential impact on troposphere–stratosphere transport (e.g., Keenan et al. 1989; Mapes and Houze 1992; Russell et al. 1993); the Maritime Continent Thunderstorm Experiment (MCTEX), focusing on the evolution of intense island-based thunderstorms (Keenan et al. 2000); the Darwin Waves Experiment, focusing on convectively generated gravity waves (Hamilton et al. 2004); and the Emerald experiment, focusing

on cirrus measurements around deep, intense storms (Whiteway et al. 2004).

The objectives of the experiment are listed in Table 1. A general theme was to document in as much detail as possible the evolution of the cloud systems in the experiment domain, the environmental controls on this evolution, and, in turn, the impact of the cloud systems on the environment. Another important component was to provide data for the validation of ground- and spaceborne remotely sensed cloud properties because these tie the experiment into long-term observational datasets in the tropics (e.g., Ackerman and Stokes 2003). The main focus of activities was within a ring of radiosonde stations established around Darwin for the experiment, although survey aircraft missions were conducted to measure the large-scale aerosol and chemical composition of the region and to sample highly aged cirrus clouds (clouds separated from their parent convection for more than 24 h) when the most active region of deep convection was located well to the south.

Table 1. Science objectives for TWP-ICE and ACTIVE.

1) Collect detailed measurements of the cirrus microphysics and relate them to storm intensity and proximity (spatial and temporal) to the parent convection.
2) Relate measurements of aerosol and chemical species in the outflow of deep convection, and in the surrounding TTL, to low-level sources, and identify how the deep convection has modified the aerosol population in the anvils.
3) Compare the concentration of aerosol and chemical tracers (with a range of lifetimes and origins) in the outflow with that in the background TTL, and therefore determine the contribution of convection to the composition of the TTL including NOX and O_3 over Darwin.
4) Improve and evaluate cloud property retrievals from satellite- and ground-based remote-sensing measurements.
5) Provide datasets for forcing and evaluating cloud-resolving and single-column models that will attempt to simulate the observed cloud system characteristics.
6) Document the evolution of oceanic convective clouds from the early convection phase through to the remnant cirrus, with particular emphasis on their microphysics.
7) Measure the dynamical and radiative impacts of the cloud systems.
8) Characterize the environment in which the cloud systems occur.
9) Document the evolution of the convective boundary layer throughout the diurnal cycle and through the life cycle of convective systems.
10) Observe the characteristics of convectively generated gravity waves.

GROUND NETWORK OBSERVATIONS.

One of the cornerstones of TWP-ICE was an extensive ground-based observational network that included long-term components as well as instruments deployed specifically for the campaign. The network spanned a region with a radius of approximately 150 km, centered on Darwin. The long-term component included the Bureau of Meteorology (BoM) instrumentation associated with meteorological research and operational forecasting applications (Keenan and Manton 1996), as well as a Department of Energy (DOE) Atmospheric Radiation Measurement (ARM) Program Atmospheric Cloud and Radiation Facility (ACRF) site (Ackerman and Stokes 2003).

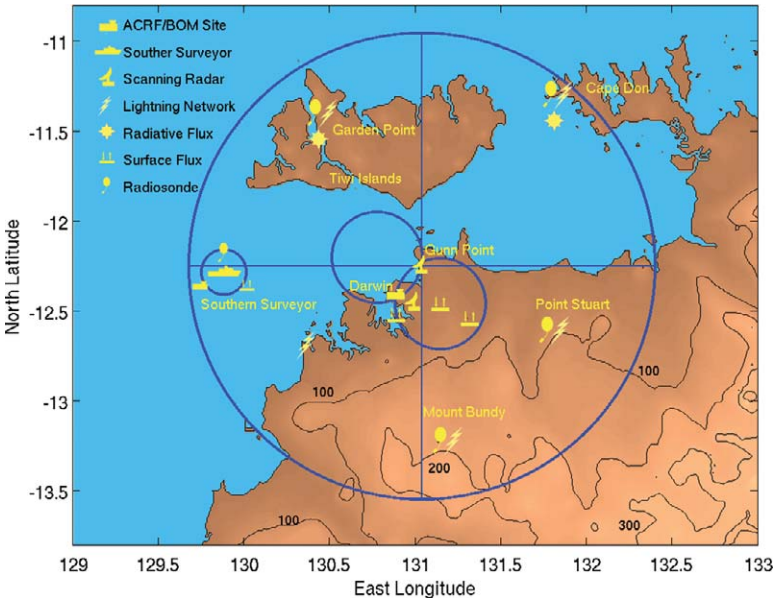

Fig. 1. The TWP-ICE/ACTIVE experiment domain. The large blue circle indicates a 150-km radius centered on the C-Pol radar. The small circle near 130°E indicates the operating region of the *Southern Surveyor*. The two interlocking circles near the center of the domain indicate the dual-Doppler lobes associated with the C-Pol and Berrima radars. Height contours are drawn every 100 m. Additional ground-based instruments are listed in Tables 2 and 3.

Additional instrumentation deployed for the campaign included a network of radiosonde sites, surface energy flux systems, radar wind and cloud profilers, multichannel microwave instruments, two Atmospheric Emitted Radiance Interferometers (AERIs), ocean observations, and a lightning detection network. Figure 1 illustrates the TWP-ICE/ACTIVE campaign region, including the location of some of these observation elements. This instrument network served multiple purposes. It provided detailed information about the meteorological environment, which was critical for mission flight planning and will be important for measurement interpretation as well as information about the vertical distribution of cloud properties, and boundary conditions for the experiment domain to aid in postexperiment model simulations.

BoM observation assets are listed in Table 2. Key instruments include a Doppler weather radar and a research polarimetric radar (Keenan et al. 1998) with a separation of approximately 25 km. This combination includes a dual-Doppler lobe over the open ocean, which allows the three-dimensional wind field to be measured within the precipitation and thicker cloud regions of the convective systems. Both radars complete a volume scan every 10 min, allowing the evolution of the anvils within complex convective systems to be followed. Thus, they provide key observations for the interpretation of other measurements. The polarimetric radar also provides a classification of the microphysical habit of hydrometeors detected by the radar (Keenan 2003; May and Keenan 2005). A Deutsche Zentrum für Luft- und Raumfahrt (DLR)

Table 2. Permanent instruments in the Darwin area associated with the Australia Bureau of Meteorology and the Department of Energy (DOE) Atmospheric Radiation Measurement (ARM) Climate Research Facility.

Instrument/system	Description
Bureau of Meteorology	
5.6-GHz scanning polarimetric radar	Provides three-dimensional hydrometeor distributions with a range of approximately 150 km, located 20 km northeast of Darwin
Operational scanning Doppler weather radar	Provides spatial distribution of convection/precipitation, located approximately 10 km southeast of Darwin
50-MHz wind profiler	Vertical profiles of wind, located 10 km southeast of Darwin
920-MHz wind profiler	Vertical profiles of wind and precipitation, located 10 km southeast of Darwin
Automated Weather Stations	Pressure, temperature, humidity, and wind speed and direction at 10 sites around the Northern Territory
Rain gauge network	
DOE ARM Climate Research Facility	
Millimeter cloud radar	35-GHz Doppler radar, provides cloud boundaries and is used to derive microphysical properties
Micropulse lidar	532-nm lidar, provides cloud boundaries and is used to derive cloud optical properties
Vaisala ceilometer	Provides cloud base to a maximum altitude of 7 km and profiles of backscatter
Total sky imager	Hemispheric digital camera provides digital snapshots of the sky and pixel-by-pixel cloud cover determination
Atmospheric Emitted Radiance Interferometer	Measures infrared emission from atmosphere in range 520–3300 cm^{-1}, with 1 cm^{-1} resolution
Microwave radiometer	23.8/31.4 GHz, provides total column water vapor and liquid water
Multifilter rotating shadow-band radiometer	Six narrowband channels between 0.4 and 1 mm provide column aerosol information
Disdrometer	Raindrop size distribution
Broadband radiometers	Up- and down-looking Eppley solar and terrestrial infrared radiometers
Surface meteorology	Pressure, temperature, humidity, rain rate, wind speed, and direction

lightning network (Betz et al. 2004) was deployed for the experiment. Lightning activity provides additional information about convective intensity and the microphysical processes occurring in the convective cores (e.g., Carey and Rutledge 2000).

Since 2002, ARM has operated an atmospheric radiation and cloud observing site in Darwin (Mather et al. 1998). The site includes measurements of the surface radiation budget, surface meteorology, and vertical distribution of clouds (Table 2). Cloud profiles are derived primarily from a pair of vertically pointing active remote sensors: a 35-GHz cloud radar [Millimeter Wavelength Cloud Radar (MMCR)] and a cloud lidar (Clothiaux et al. 2000). In addition to cloud occurrence, these instruments provide profiles of cloud microphysical properties through various retrieval algorithms (e.g., Hogan et al. 2000; Mather et al. 2007). A goal of TWP-ICE is to use in situ observations of microphysical properties to improve the retrieval of cloud properties from the long-term ground-based remote sensors at Darwin and the other tropical ARM sites. Several other profiling instruments were located at the ARM site, including a 50-MHz radar (Vincent et al. 1998), a passive microwave radiometer [Humidity and Temperature Profiling Radiometer (HATPRO); Westwater et al. 2005], as well as a 2.8-GHz profiling radar (Ecklund et al. 1999) at the nearby BoM wind profiler site (Table 3).

As mentioned above, another goal of TWP-ICE was to provide the necessary boundary conditions for model simulations. Of particular interest are high-resolution models that capture the details of convection and cirrus production, as well as single-column models that are key tools for climate model parameterization development. The observations from the BoM and ARM radars then provide the means of evaluating the modeled cloud fields. The lateral boundary conditions are derived using a network of five radiosonde sites (Fig. 1) from which balloons

Table 3. Instruments deployed in the Darwin area for TWP-ICE.

Instrument/system	Location	Description	PI/affiliation
Radiosonde array	Perimeter of TWP-ICE domain	Profiles of temperature, humidity, and wind	ACRF/Bureau/Vaisala
Flux network	Four sites over water, marsh and savannah (2)	Eddy correlation latent and sensible heat fluxes and surface radiation	Tapper (Monash University)
50-MHz profiler	Darwin ACRF site	Vertical profiles of wind	Vincent (University of Adelaide)
3-GHz profiler	Bureau profiler site	Vertical profiles of precipitation	Williams (NOAA)
Radiometer network	Garden Point and Cape Don	Downwelling broadband solar and terrestrial infrared fluxes	Long [Pacific Northwest National Laboratory (PNNL)]
LINET lightning network	Perimeter of TWP-ICE domain	Multiantenna lightning detection operating in the VLF/LF range	Hoeller (DLR)
Lightning sensor	Darwin ACRF site	VHF broadband digital interferometer for high temporal resolution lightning monitoring	Kawasaki (Osaka University)
HATPRO	Darwin ACRF site	14-channel microwave radiometer: profiles of temperature and water	Crewell (University of Munich)
Radiative fluxes	*Southern Surveyor*	Broadband solar and terrestrial infrared fluxes and SST	Reynolds [Brookhaven National Laboratory (BNL)]
Bulk fluxes	*Southern Surveyor*	Sensible and latent heat fluxes	Bradley (CSIRO)
PARSL	*Southern Surveyor*	Ceilometer, microwave radiometer, temperature, humidity, and precipitation	Mather (PNNL)
M-AERI	*Southern Surveyor*	Marine Atmospheric Emitted Radiance Interferometer	Minnett (University of Miami)
Oceanographic observations	*Southern Surveyor*	Salinity, temperature, and current profiles	Tomczak (Flinders) University)

carrying Vaisala RS-92 radiosondes were launched at 3-hourly intervals for the experiment period as well as at 6-hourly intervals at the Darwin facility. The data from these individual profiles have been integrated into an analysis of the large-scale dynamical forcing (Zhang et al. 2001). This forcing dataset also makes use of measurements of the upper and lower boundary conditions in the experiment domain, such as the experiment domain averaged precipitation derived from the BoM polarimetric radar, surface energy fluxes, and top-of-the-atmosphere and surface radiative fluxes. In support of this activity, stations measuring sensible and latent heat fluxes as well as radiative fluxes were deployed at several locations throughout the experiment domain chosen to represent a range of representative surface types from open water to savannah (e.g., Beringer and Tapper 2002). Top-of-the-atmosphere boundary conditions are provided by satellites, including the new Japanese geostationary satellite MTSAT-1R, and various polar-orbiting platforms. Cloud products associated with multiple satellites have been derived by the National Aeronautics and Space Administration (NASA) cloud and radiation support group (information online at www-pm.larc.nasa.gov).

To complement aircraft measurements of TTL composition, a program of ozonesonde launches was conducted from Darwin during the ACTIVE campaign. Most of these were launched in November and December, because of the greater focus on TTL composition compared to cloud measurements in that period (Vaughan et al. 2008), but nine were also launched during TWP-ICE. They showed a progression from a uniformly low ozone concentration (20 ppbv) during the active monsoon in mid-January to profiles in mid-February similar to those measured in the premonsoon period, with a maximum ozone mixing ratio up to 60 ppbv in the midtroposphere and a minimum <20 ppbv in the TTL. This implies a widespread vertical mixing of chemical constituents during monsoon conditions, extending from the surface to the TTL, but that at other times vertical mixing is suppressed, despite the very deep storms that deposit boundary layer material in the TTL.

Darwin is a coastal site, which means that a significant part of the experiment domain was over water. To characterize the oceanic region off the Australian coast, the Australian National Research Facility Research Vessel *Southern Surveyor,* operated by Commonwealth Scientific and Industrial Research Organisation (CSIRO), was stationed in the Timor Sea west of Darwin where it served as the base for multiple observations. Radiosondes were launched from it to complete the network of sites around the domain perimeter. The ship also carried instruments for measuring turbulent and radiative fluxes (e.g., Fairall et al. 2003), a second set of cloud remote-sensing instruments, and several instruments to measure ocean conductivity–temperature–depth (CTD) and current profiles (Godfrey et al. 1999). These measurements provide an important link between surface fluxes and the ocean mixed layer structure. Miniature CTD probes were mounted on a SeaSoar profiling platform and on three shallow moorings. In addition periodic CTD casts were made during the voyage to compare with the continuous profiles. Further aims of the ocean observations were to provide measurements of the ocean state to support both ocean and coupled modeling as well as document the impact of the convection on the structure of the upper ocean. The ocean dynamics of the ship operations area can be categorized as being somewhere between a coastal sea and the open ocean, where the combination of shallow water (50 m) and strong tides will have some influence on the mixed layer dynamics. The duration of the experiment was also long enough that tidal mixing varied significantly during the observation period. This should allow the model to isolate tidal mixing from other mixing processes, such as nighttime convection.

There are a few known data problems. There is a daytime dry bias in the soundings (Vomel et al. 2007), and a correction for this through the diurnal cycle has been developed and implemented on the datasets available through the ARM server (Hume 2007). The ARM site at Darwin suffered a lightning strike prior to the experiment and this led to a loss of sensitivity in the MMCR so that the minimum detectable signal was degraded by approximately 18 dB*Z*. At a range of 10 km, the minimum detectable signal with the reduced sensitivity was approximately –28 dB*Z*. Vibrations on the ship and high seas severely limited the shipborne radar and lidar operation, and there is little usable data from those instruments.

AIRCRAFT OBSERVATIONS AND OPERATIONS. Five research aircraft were deployed for TWP-ICE (Table 4). Flights were coordinated by a dedicated flight management team using real time four-dimensional radar visualization and satellite imagery. Two of the aircraft—the Scaled Composite's Proteus, carrying the ARM Unmanned Aerial Vehicle (UAV) suite of instruments and the Airborne Research Australia' (ARA's) Egrett—were high-altitude aircraft capable of in situ measurements in the anvil outflow.

They carried instruments for detailed microphysical and meteorological measurements, and in the case of the Egrett a suite of chemical and aerosol instrumentation. Details are given in Table 4 and the supplement (online at http://dx.doi.org/10.1175/BAMS-89-5-May) but the payloads included state measurements, aerosol and cloud particle counting and size distributions for both aircraft, and CCN, H_2O, CO, O_3, and black carbon on the Egrett as well as total water content, CO, CO_2, and radiation observations on the Proteus. The Cloud, Aerosol, Precipitation Spectrometer (CAPS) instrument on the last two flights of the Proteus were limited to sampling small crystals (D < 50 μm) for much of the flights and the aircraft was thereby operated near cloud top on 8 and 10 February. A third aircraft, a Twin Otter, carried an airborne vertically pointing 95-GHz cloud radar and lidar to support the high-altitude measurements and was flown at an altitude of about 3300 m. The remaining two aircraft were dedicated to boundary layer measurements. The Dimona measured turbulent fluxes and was primarily deployed at very low altitudes, except for some missions exploring the effect of convection on boundary layer structure and the recovery of the boundary layer after convection. The U.K. Natural Environment Research Council (NERC) Dornier aircraft carried a meteorological probe, particle size spectrometers, an aerosol mass spectrometer, and fast-response CO, O_3, and condensation nuclei, as well as a gas chromatograph and automatic tube sampler for volatile organic compound (VOC) measurements. Full details of the Dornier payload may be found in Table 2 of Vaughan et al. (2008) and a summary of the measurements are in Allen et al. (2008). This aircraft was deployed for taking areal surveys as well as partnering the Egrett in measurements of the low-level inflow and anvil outflow of convective storms.

Table 4. Aircraft Instruments and observational capabilities. Detailed tables including the aircraft instruments are available online.

Aircraft	Altitude range	Observation type
ARA Dimona	10 m–2 km	State parameters, turbulence, SW and LW radiation
NERC Dornier	100 m–4 km	State parameters, aerosol size distribution, aerosol composition, ozone, CO, hydrocarbons, and halocarbons
Twin Otter	1–3 km	NASA 96-GHz cloud radar, York University 530-nm polarization lidar
ARA Egrett	8–15 km	State parameters, upper-tropospheric humidity, cloud particle size distributions of 10 μm to ~ 1.5 mm, ice cloud particle habit, aerosol size distribution, black carbon aerosol, ozone, CO, NO_x, hydrocarbons, and halocarbons
ARM-UAV Proteus	8–16 km	State parameters, cloud particle size distributions of 10 μm to ~ 1.5 mm, cloud particle habit of 10 μm to ~ 1 mm, total water content and extinction, cloud aerosol of 0.35 to 50 μm, SW and LW radiation, 1.053-μm lidar, CO and CO_2 sensors

There were several classes of mission as outlined in Table 5. The main effort was directed toward multiaircraft missions to understand the cirrus structure and evolution. Remote-sensing observations concurrent with the in situ cloud observations were obtained from the Twin Otter flying beneath the high-altitude aircraft. There were two classes of cirrus-sampling missions. In one class, the Egrett and Proteus were directed as close as possible in space and time to fresh anvil clouds to study the microphysics, aerosol, and chemistry of the cloud being ejected from the convection and its evolution. The Dornier and Dimona were utilized in these missions to sample the boundary layer structure both ahead of the storms and in the lee. The second class of multiaircraft missions were aimed at sampling aged cirrus where the internal circulations of the cirrus and new crystal growth was dominant.

Where possible, the Proteus also performed spiral ascents and descents through the clouds over the ground- and ship-based remote-sensing sites. This has a strong link to algorithm development and validation of retrievals from the Cloudsat/Calipso satellites and long-term records at the ARM sites.

A variety of survey-type flights were undertaken in order to examine the properties of the air masses around Darwin and the spatial structure, both of the boundary layer and upper troposphere. These missions were of three basic types—low-level flux flights, flights in clear air at a number of altitudes in the Darwin area (to obtain profile information), and

Table 5. TWP-ICE Aircraft Missions. Aircraft: D = Dimona, E = Egrett, N = Dornier, P = Proteus, T = Twin Otter; cloud missions: MA = monsoon anvil, AC = aged cirrus, BA = break anvil; survey missions: L = land survey, M = maritime survey; and other missions: TO = *Terra* overpass, CO = clear-sky CO profile, I = intercomparison, Li = lidar.

Date	Cloud missions		Survey missions		Other missions	
	Aircraft	Mission	Aircraft	Mission	Aircraft	Mission
20 Jan	E N	MA				
21 Jan			D	L		
22 Jan	E N T	MA				
23 Jan	E T	MA				
25 Jan	E P T	AC	D N	L M		
26 Jan			N	L		
27 Jan	E P T	AC	N	L		
29 Jan	P T	AC	D	L		
30 Jan			N	M		
31 Jan			D	L	E	Li
1 Feb			D N	L L	E	Li
2 Feb	D P T	MA	N	L		
3 Feb			E N	M M	T	TO
4 Feb			D	M	P	CO
5 Feb			D	M		
6 Feb	E P T	BA	D	M		
8 Feb	D E N T	BA				
9 Feb	E	BA				
10 Feb	D E N P T	BA	D	M		
12 Feb	D E N P T	BA				
13 Feb	E	BA	D	L		
14 Feb					E N	I I

long-range missions at a constant altitude. Between 30 January and 3 February the Dornier flew north toward Indonesia and south to Alice Springs in central Australia. At the northern limit of these flights air with much more pollution than in Darwin was encountered, consistent with a Northern Hemisphere origin (Hamilton et al. 2007, manuscript submitted to *J. Geophys. Res.*). Far less variation was seen on the way to Alice Springs.

METEOROLOGICAL CONDITIONS. Four distinct convective regimes were sampled during the intense observing period (IOP) of TWP-ICE as a large amplitude Madden–Julian oscillation (MJO) event moved through the region. The IOP began with convectively active monsoon conditions, followed by a suppressed monsoon, 3 days of clear skies, and then a break period.[1] A series of figures will be used to illustrate the evolution of the meteorological conditions. Figure 2 shows the time accumulation of polarimetric radar estimates of the rainfall averaged over the 300-km-diameter domain that was sampled. Figure 3 shows a time–height cross section of relative humidity measured by radiosondes at Point Stuart (Fig. 1). Figure 4 shows the median convective available potential energy (CAPE) from all sounding sites (see Fig. 1 for their location), together with the area-averaged hourly rainfall throughout the TWP-ICE

[1] There are various definitions of monsoon conditions (e.g., Drosdowsky 1996), but the principal feature of the monsoon in Darwin is the presence of westerly winds between 850 and 700 hPa. The use of more complex definitions usually only change the "monsoon periods" by a few days. We will largely use a simple definition here of westerlies at 700 hPa in a 4-day smoothed wind time series, except where explicitly discussed.

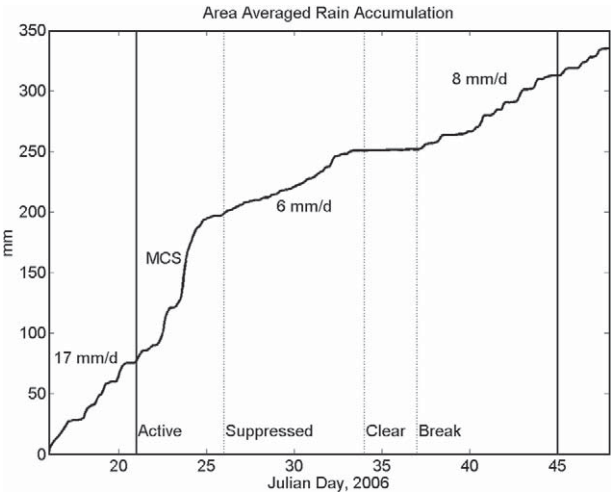

Fig. 2. Rainfall accumulation averaged over the 300-km-diameter circle sampled with the polarimetric radar. The period from 13 Jan up to 22 Jan was an active monsoon, with a major mesoscale convective system (MCS) developing on 23 Jan. The following period was a suppressed monsoon with relatively shallow storms. The transition to the break on 6 Feb was preceded by three completely clear days. The heavy vertical lines mark the beginning and end of the intensive observing period and dotted lines are regime transitions.

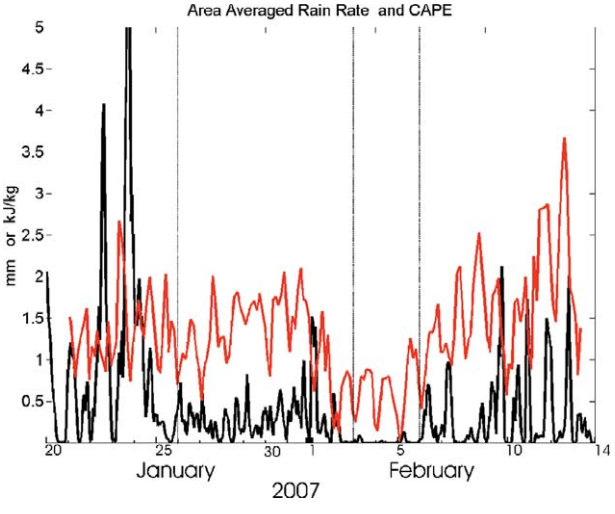

Fig. 4. Time series of area mean CAPE (red curve) and the area-averaged hourly rain rate estimated with the C-Pol radar as in Fig. 2 (black curve). The CAPE is calculated from the five sounding sites using unmodified soundings and taking the parcel from 100 m. The vertical lines mark the regime changes as in Fig. 2.

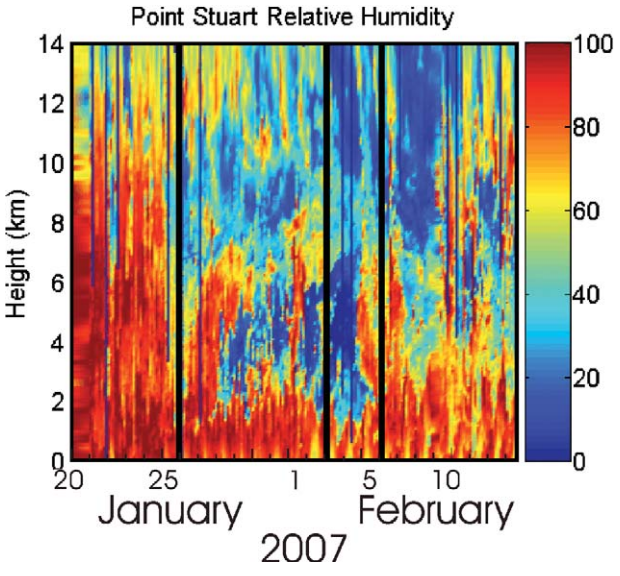

Fig. 3. Time–height cross section of relative humidity from Point Stuart radiosondes. Relative humidity is given with respect to liquid water at all altitudes. The vertical lines mark the regime changes as in Fig. 2.

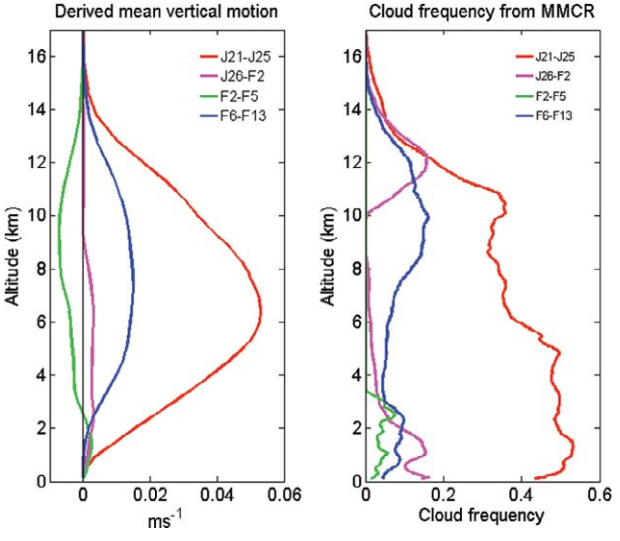

Fig. 5. Mean vertical velocity and cloud frequency profiles for the four regimes (see Fig. 2 for details). The vertical motions were calculated from the forcing dataset.

period. Figure 5 shows the mean vertical velocity profile estimated from the observational network using the methodology of Zhang et al. (2001) and the vertical distribution of clouds averaged over the three convectively active and the one suppressed period as identified by the MMCR at the ARM site in Darwin. Figure 6 highlights examples of the cloud and rainfall distribution for each of the three precipitating periods.

During the active monsoon at the beginning of the IOP the Darwin area experienced a great variety of convective organization with isolated storms, as well as lines aligned along, across, and at some angle to the shear (or all at once in a single scene). A constant feature during this period was the dense overcast

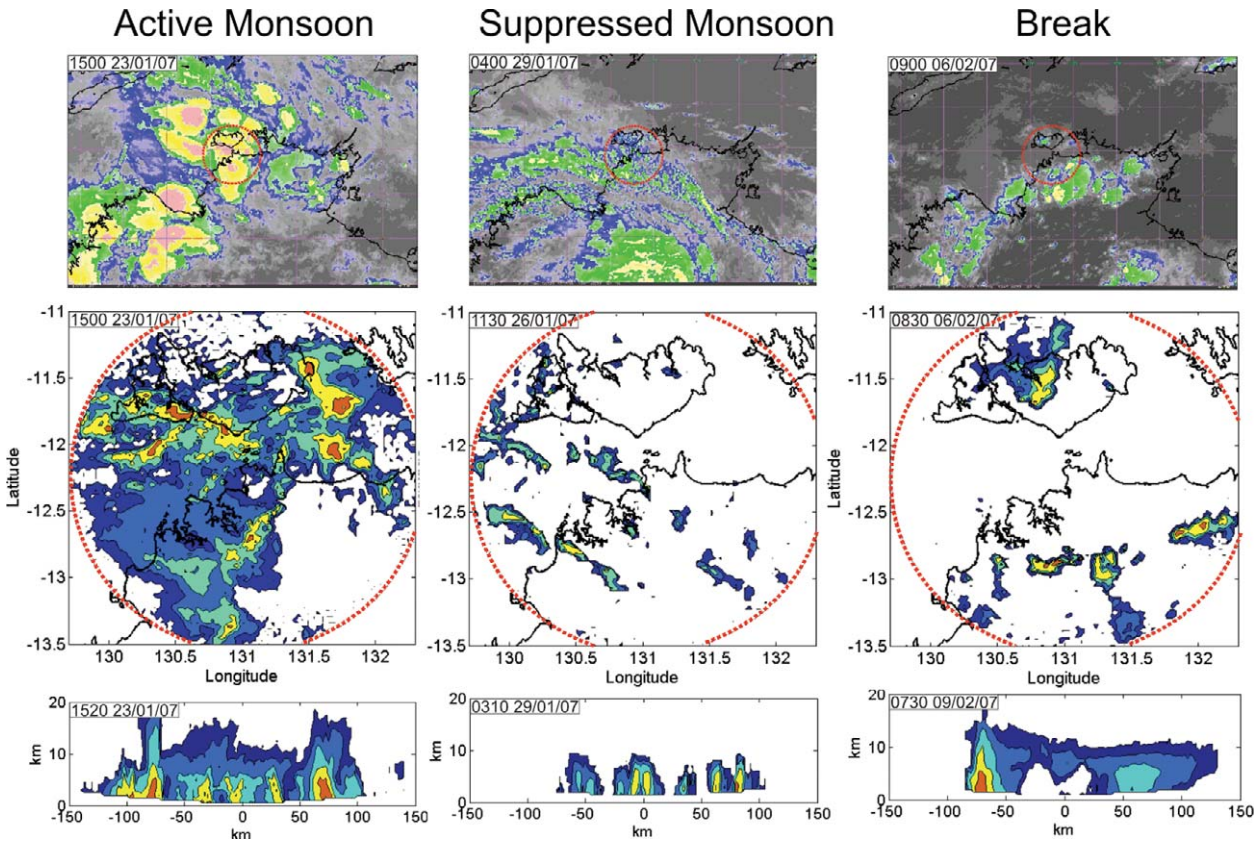

Fig. 6. Sample IR satellite images from MTSAT1-R of northern Australia, radar reflectivity maps of the experiment area and typical radar cross sections for the three rain regimes. These were (left) active monsoon, (middle) suppressed monsoons, and (right) break period. The red circles show the main experiment domain. Note that these panels are not necessarily at the same dates and times, but were rather chosen as representative of typical structure and organization observed in these periods. The IR enhancement $T > 250$ K is grayscale, 250–230 K are blue shades, 230–210 K are green shades, 210–190 K are yellow shades, and $T < 190$ are red shades. Radar contours are drawn every 10 dBZ from 10 dBZ. Dates and times are in UTC.

cirrus across the domain. Outflows from the deep convective storms were mixing with existing aged cirrus, so that cirrus sampled during this period was unlikely to be representative of either pristine new or aged anvil cirrus, except close to the convective towers. As is evident from Fig. 2, the area mean rainfall rates for this period were remarkably steady at around 17 mm day^{-1} despite widely differing levels of organization and areas covered by stratiform rain. This period was marked by high values of relative humidity throughout the troposphere (Fig. 3) and relatively high values of CAPE (Fig. 4). Consistent with the high humidity values and relatively large mean upward motion, a high frequency of cloud occurrence was detected by the MMCR throughout the column, which is by far the highest values of the TWP-ICE period. As the example in Fig. 6 (left column) shows, convection in this period was very widespread, but most individual cells were not of great intensity, with high reflectivities rarely extending much above the freezing level. However, radar echo tops still extended to about 17 km for the most intense cells (see middle row of panels of Fig. 6).

By late 23 January the monsoon trough was receding to the north of Darwin and easterly winds were being experienced at 700 hPa, although the cloud conditions and storm character were still monsoonal. A large MCS developed in the experiment region, which produced a distinct rotation as it moved across the measurement array toward the sea west of Darwin. The area-averaged rainfall rate during the passage of the MCS was about 55 mm day^{-1} (Fig. 2), with half the rain being convective in origin. The soundings immediately before the passage of the system through the experiment area showed the highest CAPE of the monsoon periods covered by TWP-ICE. This cloud system developed into a tropical low and would almost certainly have become a tropical cyclone had it not made landfall to the southwest of Darwin at a central pressure of 999 hPa.

The low continued to intensify, eventually deepening to 988 hPa over the land on 31 January. It established itself as an almost stationary feature over the central part of the Northern Territory until 2 February. Its intensity and spiral cloud structure led to it being informally dubbed "Landphoon John." Widespread deep convection and torrential rain associated with this low brought extensive flooding to the semiarid lands south of Darwin.

The presence of this cyclonic center to the south had several impacts on the cloud systems around Darwin. Its circulation sustained surface westerly winds of more than 20 m s^{-1} across the Darwin area and adjacent waters, but also advected very dry continental air over the experimental area at midlevels (Fig. 3). This had the effect of limiting storm heights during this period to below 10 km so it was atypical of "normal" monsoon conditions. The organization of convection ranged from isolated cells to short lines, but with no significant stratiform cloud. The upward vertical velocity was confined to the lower levels with descending motion aloft. While CAPE remained high (Fig. 4), observed rain rates were much lower (5–7 mm day^{-1}), which is likely attributable to the drier and subsiding middle and upper troposphere. The vertical cloud distribution during this period shows two distinct peaks in the lower and upper troposphere (purple line, Fig. 5). The maximum at the upper levels was due to advection of cirrus northward from the cyclone center to the south. Most of the experiment area was covered by relatively low clouds. The radar images indicate mostly shallow rain features, although individual small cells reaching the 10-km level were observed. This period experienced the cleanest low-level air measured during the campaign with less than 50 ppbv of CO and one aerosol particle per cubic centimeter in the size range > 300-nm diameter.

The low pressure system to the south dissipated rapidly on 3 February, and 3 days of clear skies and no precipitation were experienced at Darwin. These days were associated with the lowest CAPE throughout the experiment (Fig. 4) and showed the driest conditions above the boundary layer measured in TWP-ICE (Fig. 3) associated with the mean descending motion (Fig. 5). Consistent with these conditions the cloud radar observed hardly any cloud (green line, Fig. 5).

With the dissipation of the intense low to the south, conditions in the experiment area changed to those typical of a break period with easterly flow throughout the column. As is typical in such cases, convection during this period exhibited intense afternoon thunderstorms, and some squall lines passing Darwin at night. These lines had their genesis in the previous afternoon's convection to the east. Despite the great intensity of the individual thunderstorms, area mean rainfall during this period was only around 8 mm day^{-1} due to their relatively small coverage (in space and time) compared to the active monsoon conditions (Fig. 2). The period was accompanied by a gradual moistening of the middle and upper troposphere (Fig. 3) and a gradual increase of CAPE (Fig. 4), culminating in the largest values of CAPE observed toward the very end of the experiment. The lower mean vertical motion compared to the active monsoon (Fig. 5) is consistent with the lower mean rain rates, but the upward motion does extend slightly higher in the break. Significant amounts of upper-level cloud associated with the convection were observed by the MMCR in this period (blue line, Fig. 5), but much less than during the active monsoon (red curve).

It is interesting to contrast the distribution of upper-level clouds during the suppressed monsoon period (26 January–2 February) and the break period (6 February through the end of the experiment). The depth of the cirrus layer was limited to altitudes above 10 km during the earlier period when the middle troposphere was very dry (Fig. 3), but the cirrus layer was much deeper during the break period consistent with the moister conditions. It is evident from the examples shown in Fig. 6 that convection during this period was of a strongly continental character and was often related to mesoscale circulation features, such as the sea breeze. The radar images (third column, Fig. 6) exemplify the high intensity of the convection, with reflectivities above 35 dBZ extending above 15 km on a regular basis. This was accompanied by strong electrical activity, which was virtually absent in the earlier monsoon convection.

The convective regimes observed during TWP-ICE and described above constitute typical examples of continental and maritime convection observed elsewhere in the tropics (e.g., Keenan and Carbone 1992), while the relatively shallow but intense convection in the suppressed regime is somewhat unusual, and will be a strong test for models. While a longer sample of active monsoon convection would have been desirable, the TWP-ICE dataset is a significant resource for the study of these convective regimes. Opportunities for such studies will be highlighted in the next sections.

A SAMPLE OF THE OBSERVATIONS AND RELATED SCIENCE QUESTIONS. The science objectives listed in Table 1 include relating cirrus properties to the convective intensity and to aerosol

properties, providing validation for remote-sensing retrievals, and collecting a dynamical forcing dataset for cloud modeling. Applications of the data to some of these goals is described in this section.

The experiment array was designed to support modeling activities and provide boundary conditions for a range of model activities with a focus on single-column and cloud-resolving models. Model forcing datasets calculated using the methodology of Zhang et al. (2001) are available based on the analysis of radiosonde, radar, and flux data (online at http://iop.archive.arm.gov/arm-iop/2006/twp/twp-ice/xie-klein-forcing/). These also provide a detailed view of the diurnal cycle and evolution of the atmosphere at high temporal resolution, while turbulent and radiative fluxes over a variety of surface types provide a detailed description of the surface energy balance.

The evolution of boundary layer aerosol during the course of this experiment and its premonsoon partner described in the companion paper (Vaughan et al. 2008) provides an opportunity to study the effects of aerosol on deep convection. Similar meteorological conditions prevailed at the beginning of November 2005 prior to the monsoon onset and in mid-February at the end of TWP-ICE—land-based afternoon convection triggered by sea breezes, exemplified by the afternoon storms on the Tiwi Islands. However, the boundary layer aerosol characteristics were markedly different. The Dornier measurements showed a transition from copious biomass-burning products (including black carbon) in mid-November, to cleaner conditions in December (Vaughan et al. 2008), and extremely clean conditions in the suppressed monsoon period when maritime air of Southern Hemisphere midlatitude origin reached Darwin. Although accumulation mode aerosol amounts were higher in the subsequent break period, they were still a factor of 2 less than in the premonsoon period. Their composition was dominated by the organic fraction in the monsoon break (as in the premonsoon period), but during the active monsoon these aerosols were predominantly sulfate. Larger aerosols (diameter > 1 μm) were around 5–10 times more prevalent in the monsoon periods than during the premonsoon and break, consistent with production of sea salt by the strong monsoonal westerlies. Such aerosols form very effective cloud condensation nuclei and modeling studies are currently under way to examine the impact of the different aerosol regimes on deep convection.

The comprehensive dataset provides opportunities and challenges for the modeling community. Just as important as the high-time-resolution forcing data are the measurements from the aircraft and remote-sensing instruments [e.g., C-band dual-polarization Doppler radar (CPOL) profilers, ARM suite], which constrain factors ranging from broad-scale characteristics of the convective systems to the details of microphysical parameterizations. The various meteorological and aerosol regimes that were sampled will provide an additional challenge: Can the models represent these differences, and how do they compare with observations? For example, it has been shown that models have particular difficulties representing convection reaching to the midtroposphere only, as observed during the suppressed monsoon (Inness et al. 2001).

The variations in weather regime during the experiment sets the scene for studying cirrus properties in relation to convective intensity and variations in boundary layer characteristics. The cirrus properties of several anvils within the sounding array were sampled in both the monsoonal and break periods

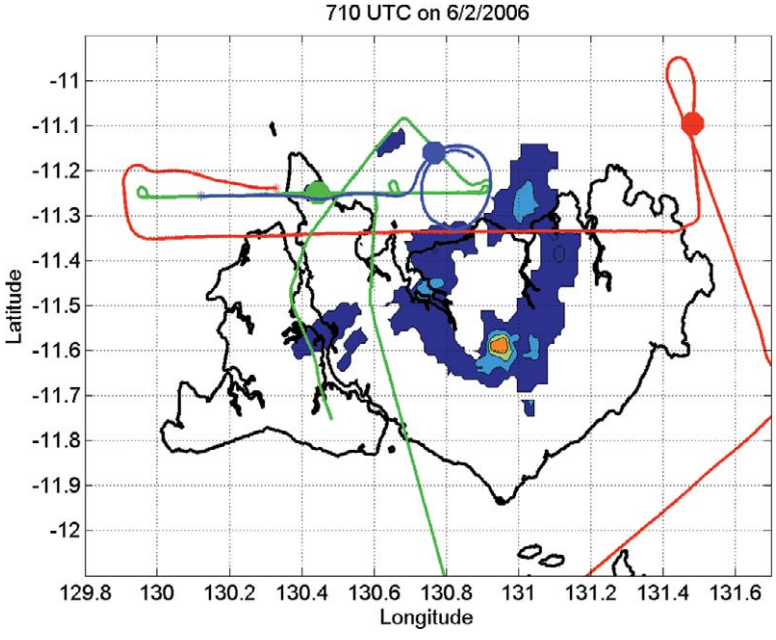

Fig. 7. Rain map from the polarimetric radar at 0710 UTC 6 Feb 2006. Contours are drawn every 20 mm h^{-1} from 0 mm h^{-1}. Aircraft tracks from the Twin Otter (green), Egrett (red), and Proteus (blue) are overlaid. The circles mark the aircraft position and tracks are drawn for +/– 1 h around the radar scan time (0710 UTC) for the Twin Otter and Egrett and +/– 10 min for the Proteus.

(Table 5), allowing the cirrus microphysics to be related to parent storm intensity. Preliminary indications are that the monsoon cirrus was characterized by both larger mean sizes and higher ice water contents than break period storms (A. Heymsfield 2007, personal communication).

An illustration of the approach and data for studying anvils is shown in Figs. 7–9. Break conditions were established by 6 February, with easterly flow at 700 hPa overlying westerlies at the surface. An isolated single-cell storm broke out over the northeast of the Tiwi Islands around 0450 UTC, with radar echoes reaching 17 km. It produced a detached anvil, which was advected northwestward over the next 2 h. The flight strategy and accompanying rain field is shown in Fig. 7. The Proteus was first on station performing two spirals through the anvil between 11- and 15-km altitude and then lining up for straight transects stacked with the Egrett and Twin Otter with the high-altitude aircraft legs between 11.2 and 14.1 km. At the lower level the Dornier flew around the storm at 300 and 800 m after first making a detailed survey of its inflow (western) side. This day provides an excellent example of a single-cell island thunderstorm developing in low-aerosol conditions, in contrast with the more polluted higher aerosol example of 16 November (Vaughan et al. 2008). Figure 8 shows a representative sample of cloud particle imager (CPI) images as a function of altitude for the descending spiral at 0700 UTC showing the presence of plate-like, irregular, and aggregates of plate-like crystals. An automated shape analysis using various measures of crystal morphology showed that irregular particles dominated the population of particles with $D > 100\ \mu$m, irrespective of altitude. Particles with $D < 100\ \mu$m were dominantly quasi spherical and made significant contributions to the total mass and optical extinction.

The observations in the fresh anvil microphysics can be contrasted with observations in aged cirrus obtained during the project. For example, on 29 January 2006 the Proteus flew constant-altitude legs to measure the latitudinal dependence of the microphysical properties of cirrus bands with minimum ages of approximately 4 h generated by a low pressure system south of the TWP-ICE domain. As with the case of aged cirrus, crystals with $D < 100\ \mu$m were predominantly quasi spherical in shape and typically contributed more

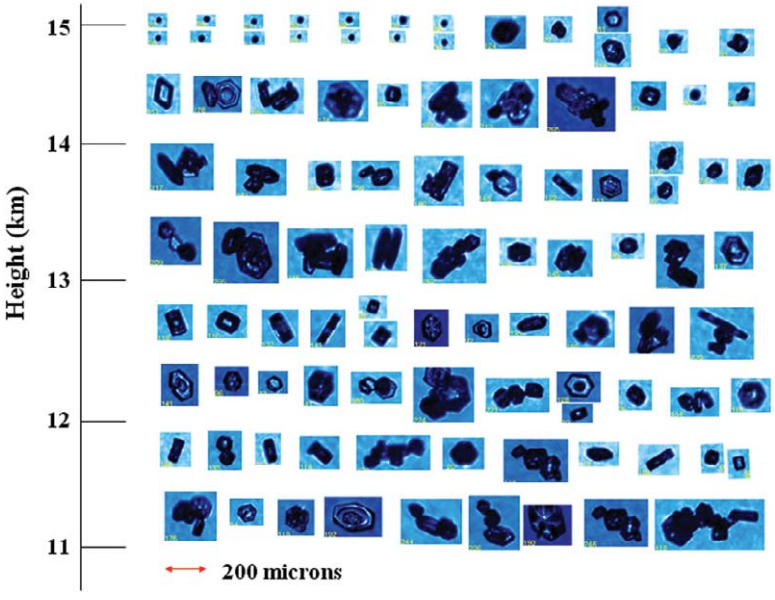

Fig. 8. SPEC CPI images of ice crystals with $D > 100\ \mu$m from a spiral descent through a fresh break period thunderstorm anvil from 6 Feb 2006 showing a mixture of quasi spherical and chain crystal habits sorted by altitude (Courtesy of J. Um, University of Illinois).

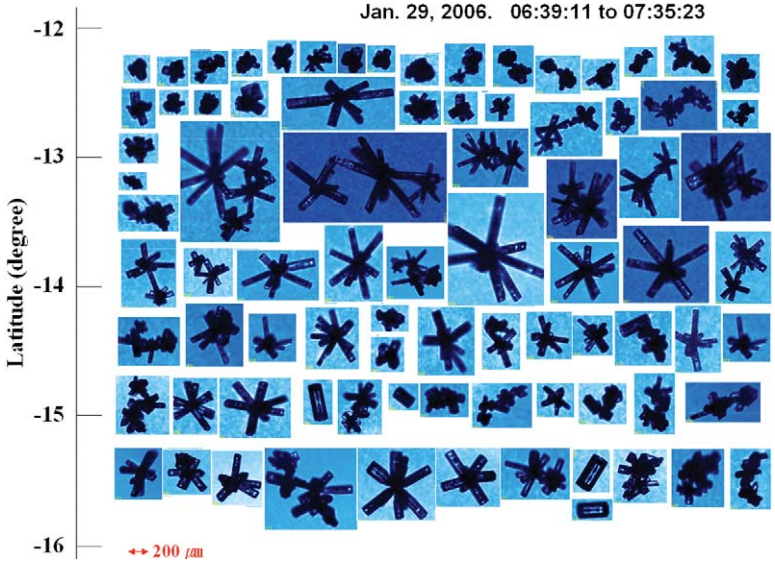

Fig. 9. CPI images of ice crystals with $D > 100\ \mu$m in an aged anvil at an altitude of 12 km on 29 Jan sorted by time showing large numbers of bullet rosettes.

than half to the total mass and extinction. On the other hand, there were differences in the shapes of large crystals compared to the aged cirrus. Figure 9 shows ice crystals imaged by the CPI with $D > 100\ \mu$m. Pristine shapes, such as bullet rosettes or aggregates of bullet rosettes, appeared regardless of altitude for these cirrus bands, which represents a strong contrast to the plates and aggregates seen in Fig. 8. The automated habit classification scheme showed that bullet rosettes dominated the population of crystals with $D > 100\ \mu$m. The difference in crystal habits between fresh anvils and aged anvils gives information about formation mechanisms/growth histories of crystals in different cloud genre. For example, the bullet rosettes in the aged anvils indicate that new particle formation is occurring in regenerating cells. Knowledge of the variation of crystal habits with cloud age gives data needed to develop, improve, and evaluate algorithms to retrieve cloud microphysical properties from ground-based remote sensors that will ultimately be used to obtain larger datasets of cloud properties.

The data from all the microphysical probes are now being used to estimate the size and shape distributions of ice crystals and to estimate their bulk mass and single-scattering properties of the cirrus following McFarquhar and Heymsfield (1996) and McFarquhar et al. (2002). The microphysical data are being placed in meteorological context to better understand how the characteristics of the convection affect the sizes, shapes, and number densities of the cloud particles. This will be used to improve the assumptions used in satellite- and ground-based remote-sensing algorithms. Spiral ascents and descents performed over the ACRF site at Darwin and the Twin Otter are providing the needed verification data for the remotely sensed microphysical retrievals of both ground- and space-based observations such as Cloudsat and Calipso. Importantly, a comparison of data from probes on the Proteus suggest that shattering large ice crystals on the protruding components of one of the probes may have artificially amplified small crystal concentrations (McFarquhar et al. 2007). This direct evidence for amplified concentrations due to crystal shattering is a significant finding, because quantifying the contribution of such small crystals to the mass and radiative properties of cirrus represents a controversial and unsolved problem in cloud physics, yet has a critical impact on determining how cirrus affects radiative heating.

As well as the planned components, the weather that was sampled also provides a number of unanticipated research opportunities. These include the sampling of surface fluxes over warm tropical oceans at high wind speeds over several days. This dataset has clear applications in the study of the formation of intense tropical weather systems forced by surface fluxes, such as tropical cyclones. Other systems that were sampled include a large MCS that developed distinct rotation within the experiment domain. There is little doubt that this system would have spawned a tropical cyclone if it had remained over warm water instead of making landfall, so again there are opportunities to look at the early stages of tropical cyclogenesis. The mature cyclone brought Southern Ocean midlatitude air to Darwin, and survey flights of the Dornier and Egrett northeastward during this period measured the transition between this very clean air and air of Indonesian, and even Northern Hemispheric origin with much higher concentrations of CO and particulates (Hamilton et al. 2007, manuscript submitted to *J. Geophys. Res.*). Even data from the suppressed period near the middle of the campaign will be useful. During this period, clear-sky radiative fluxes were obtained along with vertical profiles of temperature and humidity undisturbed by convection. These observations provide a very useful baseline for measurements obtained under other conditions.

CONCLUDING COMMENTS. TWP-ICE has succeeded in collecting an outstanding dataset describing tropical cloud systems, their evolution, and their interaction with the larger environment. The observations taken during TWP-ICE should be viewed in the context of long-term observations of clouds using remote-sensing techniques that are also available via the ARM Web site (online at www.arm.gov). Data taken during the experiment include several tens of spiral ascents over the ground and airborne cloud radar–lidar combinations. These observations will serve as a valuable resource for both the development and validation of retrieval techniques, as well as place the TWP-ICE observations in long-term statistical contexts. The experiment documented the cloud systems in a range of convective regimes and the experiment design assures a quality dataset for providing boundary conditions for simulations as well as detailed validation. These provide the core datasets for budget studies and parameterization development using a range of modeling and data analysis approaches.

The TWP-ICE datasets is a resource for the entire meteorological community. It is significant in terms of the range and completeness of the observations

of tropical cloud processes. Much of the data are already available to the community through the ARM Web site (online at www.archive.arm.gov/) as an IOP dataset while U.K.-supported aircraft data (Egrett and Dornier) will be made public in early 2008.

ACKNOWLEDGMENTS. TWP-ICE and ACTIVE were supported under the auspices of the U.S. Department of Energy ARM Program, the ARM Unmanned Aerial Vehicle Program, NASA Cloudsat, the U.K. Natural Environment Research Council Grant NE/C512688/1, the NERC Airborne Remote Sensing Facility, the Australian National Marine Research Facility, the Australian Bureau of Meteorology, and the Kyoto University Active Geosphere Investigation (KAGI) for the twenty-first-century COE program. Vaisala generously donated the radiosonde base stations. The Charles Darwin University, Darwin RAAF Base, and Tiwi Island Land Council all made extensive facilities available to the experiment. More than 100 scientists were in the field. Particular thanks are due to retired Bureau of Meteorology observers, who led the operations of the remote-sounding sites. Without the cooperation of a large team of specialists this experiment would not have been possible. We thank, in particular, the pilots, aircraft scientists, and ground crew of the five aircraft for ensuring that the missions were so successful, and the staff of the Bureau of Meteorology Regional Centre in Darwin for their invaluable support both for forecasting and logistics. The whole experiment team is indebted to Brad Atkinson, Anthony Noonan, Tim Hume, Andrew Hollis, and Lori Chappel whose untiring efforts made the experiment possible. Data were obtained from the ARM program archive, sponsored by DOE, Office of Science, Office of Biological and Environmental Research, Environmental Science Division. The forcing dataset was derived by a collaboration between M.-H. Zhang and S. Xie of Los Alamos National Laboratory and Tim Hume of BMRC.

REFERENCES

Ackerman, T. P., and G. Stokes, 2003: The Atmospheric Radiation Measurement Program. *Phys. Today,* **56,** 38–45.

Allen, G., and Coauthors, 2008: Aerosol and trace-gas measurements in the Darwin area during the wet season, *J. Geophys. Res.,* **113,** D06306, doi:10.1029/2007JD008706

Beringer, J., and N. Tapper, 2002: Surface energy exchanges and interactions with thunderstorms during the Maritime Continent Thunderstorm Experiment (MCTEX). *J. Geophys. Res.,* **107,** 4552, doi:10.1029/2001JD001431.

Betz, H.-D., K. Schmidt, P. Oettinger, and M. Wirz, 2004: Lightning detection with 3-D discrimination of intracloud and cloud-to-ground discharges. *Geophys. Res. Lett.,* **31,** L11108, doi:10.1029/2004GL019821.

Blossey, P. N., C. S. Bretherton, J. Cetrone, and M. Kharoutdinov, 2007: Cloud resolving model simulations of KWAJEX: Model sensitivities and comparisons with satellite and radar observations. *J. Atmos. Sci.,* **64,** 1488–1508.

Carey, L. D., and S. A. Rutledge, 2000: The relationship between precipitation and lightning in tropical island convection: A C-band polarimetric radar study. *Mon. Wea. Rev.,* **128,** 2687–2710.

Cecil, D. J., S. J. Goodman, D. J. Boccippio, E. J. Zipser, and S. W. Nesbit, 2005: Three years of TRMM precipitation features. Part I: Radar, radiometric, and lightning characteristics. *Mon. Wea. Rev.,* **133,** 543–566.

Clothiaux, E. E., T. P. Ackerman, G. G. Mace, K. P. Moran, R. T. Marchand, M. A. Miller, and B. E. Martner, 2000: Objective determination of cloud heights and radar reflectivities using a combination of active remote sensors at the ARM CART sites. *J. Appl. Meteor.,* **39,** 645–665.

DelGenio, A. D., and W. Kovari, 2002: Climatic properties of tropical precipitating convection under varying environmental conditions. *J. Climate,* **15,** 2597–2615.

Drosdowsky, W., 1996: Variability of the Australian summer monsoon at Darwin: 1957–1992. *J. Climate,* **9,** 85–96.

Ecklund, W. L., C. R. Williams, P. E. Johnston, and K. S. Gage, 1999: A 3-GHz profiler for precipitating cloud studies. *J. Atmos. Oceanic Technol.,* **16,** 309–322.

Fairall, C. W., E. F. Bradley, J. E. Hare, A. A. Grachev, and J. B. Edson, 2003: Bulk parameterization of air–sea fluxes: Updates and verification for the COARE algorithm. *J. Climate,* **16,** 571–591.

Folkins, I., 2002: Origin of lapse rate changes in the upper tropical troposphere. *J. Atmos. Sci.,* **59,** 992–1005.

Garrett, T. J., and Coauthors, 2005: Evolution of a Florida cirrus anvil. *J. Atmos. Sci.,* **62,** 2352–2372.

Godfrey, J. S., E. F. Bradley, P. A. Coppin, L. F. Pender, T. J. McDougall, E. W. Schulz, and I. Helmond, 1999: Measurements of upper ocean heat and freshwater budgets near a drifting buoy in the equatorial Indian Ocean. *J. Geophys. Res.,* **104** (C6), 13 269–13 302.

Greenfield, R. S., and T. N. Krishnamurti, 1979: The Winter Monsoon Experiment—Report of December 1978 field phase. *Bull. Amer. Meteor. Soc.,* **60,** 439–444.

Hamilton, K., R. A. Vincent, and P. T. May, 2004: Darwin Area Wave Experiment (DAWEX) field campaign to study gravity wave generation and propagation. *J. Geophys. Res.,* **109,** D20S01, doi:10.1029/2003JD004393.

Heymsfield, A. J., and G. M. McFarquhar, 1996: High albedos of cirrus in the tropical Pacific Warm pool: Microphysical interpretations from CEPEX and from Kwajalein, Marshall Islands. *J. Atmos. Sci.,* **53,** 2424–2451.

——, Z. Wang, and S. Matrosov, 2005: Improved radar ice water content retrieval algorithms using coincident microphysical and radar measurements. *J. Appl. Meteor.,* **44,** 1391–1412.

Hogan, R. J., A. J. Illingworth, and H. Sauvageot, 2000: Measuring crystal size in cirrus using 35- and 94-GHz radars. *J. Atmos. Oceanic Technol.,* **17,** 27–37.

Höglund, S., 2005: Clouds in Darwin and their relation to large-scale conditions. M.S. thesis, Dept. of Applied Physics and Mechanical Engineering, Lulea University of Technology, 52 pp. [Available online at http://epubl.ltu.se/1402-1617/2005/169/index-en.html.]

Holland, G. J., J. L. McBride, R. K. Smith, D. Jasper, and T. D. Keenan, 1986: The BMRC Australian Monsoon Experiment: AMEX. *Bull. Amer. Meteor. Soc.,* **67,** 1466–1472.

Houze, R. A., Jr., and A. K. Betts, 1981: Convection in GATE. *Rev. Geophys. Space Phys.,* **19,** 541–576.

Hume, T., 2007: Radiation dry bias in the TWP-ICE radiosonde soundings. *Proc. 17th ARM Science Team Meeting,* Monterey, CA, ARM. [Available online at www.arm.gov/publications/proceedings/conf17/poster/P00011.pdf.]

Inness, P. M., J. M. Slingo, S. J. Woolnough, R. B. Neale, and V. D. Pope, 2001: Organization of tropical convection in a GCM with varying vertical resolution: Implications for the simulation of the Madden–Julian Oscillation. *Climate Dyn.,* **17,** 777–793.

Jakob, C., and G. Tselioudis, 2003: Objective identification of cloud regimes in the Tropical Western Pacific. *Geophys. Res. Lett.,* **30,** 2082, doi:10.1029/2003GL018367.

Keenan, T. D., 2003: Hydrometeor classification with a C-band polarimetric radar. *Aust. Meteor. Mag.,* **52,** 23–31.

——, and R. E. Carbone, 1992: A preliminary morphology of precipitation systems in tropical northern Australia. *Quart. J. Roy. Meteor. Soc.,* **118,** 283–326.

——, and M. J. Manton, 1996: Darwin climate monitoring and research station: Observing precipitating systems in a monsoon environment. BMRC Research Rep. 53, 31 pp.

——, J. McBride, G. Holland, N. Davidson, and B. Gunn, 1989: Diurnal variations during the Australian Monsoon Experiment (AMEX) Phase II. *Mon. Wea. Rev.,* **117,** 2535–2553.

——, K. Glasson, F. Cummings, T. S. Bird, J. Keeler, and J. Lutz, 1998: The BMRC/NCAR C-band polarimetric (C-Pol) radar system. *J. Atmos. Oceanic Technol.,* **15,** 871–886.

——, and Coauthors, 2000: The Maritime Continent Thunderstorm Experiment (MCTEX): Overview and some results. *Bull. Amer. Meteor. Soc.,* **81,** 2433–2455.

Mapes, B., and R. A. Houze Jr., 1992: An integrated view of the 1987 Australian monsoon and its mesoscale convective systems. Part 1: Horizontal structure. *Quart. J. Roy. Meteor. Soc.,* **118,** 927–963.

Mather, J. H., Tp. P. Ackerman, W. E. Clements, F. J. Barnes, M. D. Ivey, L. D. Hatfield, and R. M. Reynolds, 1998: An Atmospheric Radiation and Cloud Station in the tropical western Pacific. *Bull. Amer. Meteor. Soc.,* **79,** 627–642.

——, S. A. McFarlane, M. A. Miller, and K. L. Johnson, 2007: Cloud properties and associated heating rates in the tropical western Pacific. *J. Geophys. Res.,* **112,** D05201, doi:10.1029/2006JD007555.

May, P. T., and T. D. Keenan, 2005: Evaluation of microphysical retrievals from polarimetric radar with wind profiler data. *J. Appl. Meteor.,* **44,** 827–838.

——, and A. Ballinger, 2007: The statistical characteristics of convective cells in a monsoon regime (Darwin, Northern Australia). *Mon. Wea. Rev.,* **135,** 82–92.

McFarquhar, G. M., and A. J. Heymsfield, 1996: Microphysical characteristics of three anvils sampled during the Central Equatorial Pacific Experiment. *J. Atmos. Sci.,* **53,** 2401–2423.

——, P. Yang, A. Macke, and A. J. Baran, 2002: A new parameterization of single-scattering solar radiative properties for tropical ice clouds using observed ice crystal size and shape distributions. *J. Atmos. Sci.,* **59,** 2458–2478.

——, J. Um, M. Freer, D. Baumgardner, G. L. Kok, and G. Mace, 2007: Importance of small ice crystals to cirrus properties: Observations from the Tropical Warm Pool International Cloud Experiment (TWP-ICE). *Geophys. Res. Lett.,* **34,** L13803, doi:10.1029/2007GL029865.

Neale, R., and J. Slingo, 2003: The maritime continent and its role in the global climate: A GCM study. *J. Climate,* **16,** 834–848.

Nesbitt, S. W., R. Cifelli, and S. A. Rutledge, 2006: Storm morphology and rainfall characteristics of TRMM precipitation features. *Mon. Wea. Rev.,* **134,** 2702–2721.

Russell, P. B., L. Phister, and H. B. Selkirk, 1993: The Tropical Experiment of the Stratosphere–Troposphere Exchange Project (STEP): Science objectives, operations, and summary findings. *J. Geophys. Res.,* **98,** 8563–8589.

Spencer, H., and J. M. Slingo, 2003: The simulation of peak and delayed ENSP teleconnections. *J. Climate,* **16,** 1757–1774.

Stephens, G. L., 2005: Cloud feedbacks in the climate system: A critical review. *J. Climate,* **18,** 237–273.

Vaughan, G., and Coauthors, 2008: SCOUT-03/ACTIVE: High-altitude aircraft measurements around deep tropical convection. *Bull. Amer. Meteor. Soc.,* **89,** 647–662.

Vincent, R. A., S. Dullaway, A. MacKinnon, I. M. Reid, F. Zinc, P. T. May, and B. Johnson, 1998: A VHF boundary layer radar: First results. *Radio Sci.,* **33,** 845–860.

Vomel, H., and Coauthors, 2007: Radiation dry bias of the Vaisala RS92 humidity sensor. *J. Atmos. Oceanic Technol.,* **24,** 953–963.

Webster, P. J., and R. A. Houze Jr., 1991: The Equatorial Mesoscale Experiment (EMEX): An overview. *Bull. Amer. Meteor. Soc.,* **72,** 1481–1505.

——, and R. Lukas, 1992: TOGA COARE: The Coupled Ocean–Atmosphere Response Experiment. *Bull. Amer. Meteor. Soc.,* **73,** 1377–1416.

Westwater, E. R., S. Crewell, and C. Mätzler, 2005: Surface-based microwave and millimeter wave radiometric remote sensing of the troposphere: A tutorial. *IEEE Geoscience and Remote Sensing Newsletter,* March, 16–33. [Available online at www.grss-ieee.org.]

Whiteway, J., and Coauthors, 2004: Anatomy of cirrus clouds: Results from the Emerald airborne campaigns. *Geophys. Res. Lett.,* **31,** L24102, doi:10.1029/2004GL021201.

Yuter, S., R. A. Houze, E. A. Smith, T. T. Wilheit, and E. Zipser, 2005: Physical characterization of tropical oceanic convection observed in KWAJEX. *J. Appl. Meteor.,* **44,** 385–415.

Zhang, M. H., J. L. Lin, R. T. Cederwall, J. J. Yio, and S. C. Xie, 2001: Objective analysis of ARM IOP data: Method and sensitivity. *Mon. Wea. Rev.,* **129,** 295–311.